

Chamfer Masks: Discrete Distance Functions, Geometrical Properties and Optimization

Edouard Thiel and Annick Montanvert

Equipe RFMQ - TIM3 - IMAG; CNRS USRB 00690; Université Joseph Fourier
 CERMO - BP 53X - 38041 GRENOBLE CEDEX - FRANCE
 tél. (33) 76 51 48 13 - fax: (33) 76 51 49 48
 e-mail: thiel@orange.imag.fr - montanv@imag.imag.fr

Abstract

In this paper, we are interested in discrete distance functions and more precisely in the chamfer distances. These distances are based on the definition of masks whose size can change depending on the quality of the approximation which is expected, compared to the Euclidean distance. We show the induced geometrical properties of the generated distance images, and calculate the required properties of the mask to ensure that they define a distance function. Then we present how to optimize the masks directly in discrete space, and finally, we show some main applications.

1 - Chamfer Masks and Distances

In image analysis measuring distances between objects is often essential. Because acquisition devices and images are based on sampling and quantitation, and computers process discrete information, the data are also discrete, and consequently we prefer distances which generate integer values.

Since the Euclidean distance d_E gives floating numbers, and neither $(d_E)^2$ nor $\text{Round}(d_E)$ defines a distance in the mathematical sense, we will not use them.

Working on the square lattice, the well-known d_4 (City Block) and d_8 (Chessboard) distances are easy to compute [10], but they are not isotropic. This leads to some errors in many applications, for instance the separation of cell aggregates. We will not consider the octagonal distance which differs from d_E less than d_8 , but cannot be improved.

Two categories of distances hold our attention: *rational distances* [8], precursors of the *chamfer distances* family [4].

U. Montanari introduced distances where a few displacements are weighted with the equivalent Euclidean distance values. The selected points are chosen among the *visible* points of the square lattice (that is the points whose coordinates are prime factors between them), and the value of any other point is assigned with the *minimal path* through the so defined network to reach it. Analytical

expressions are computed with the Farey series of integers [6].

The main disadvantage is the use of rational numbers. G. Borgefors adapted them to the discrete space, approaching square roots by fractions (for example $1, \sqrt{2}, \sqrt{5}$ by $1, 7/5, 11/5$). In this case, a chamfer mask depicts the weighted distances (see Figure 1); it is 8-symmetrical and thus defined by the first octant.

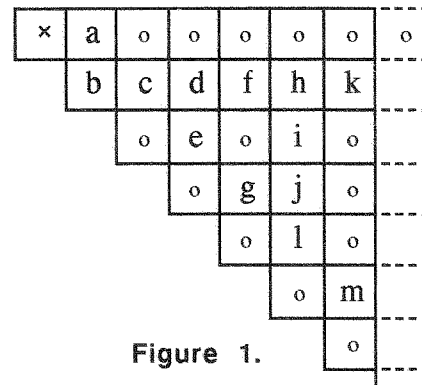


Figure 1.

We call a, b, c, \dots the visible points. For examples: $a=3, b=4$, in a 3×3 mask, and $a=5, b=7, c=11$ in a 5×5 mask.

2 - Theoretical Study

These chamfer masks have been existing for ten years, but no one took any interest to demonstrate that such a mask induces a distance in mathematical sense (triangular inequality and separability), and more generally, to obtain the exact constraints between the values a, b, c, \dots in the selected neighbourhood.

We name M_1, M_2, \dots the n affected points in the first octant of the mask, sorted out by increasing angles with (Ox) line (remark: $M_1 = a$ and $M_n = b$). We note $|M_i|$ the weight and $\|M_i\| = \sqrt{x_i^2 + y_i^2}$. This order corresponds exactly with Farey series $y_i/x_i < y_{i+1}/x_{i+1}$.

An *influence cone* is the set of pixels between the lines (O, M_i) and (O, M_{i+1}) .

Theorem 1:

In an influence cone M_i/M_{i+1} , the only points of the mask which are necessary to find of the minimum for computing the distance from O are the local distances $|M_i|$ and $|M_{i+1}|$:

- By shifting, $|M_i|$ provides the values $2|M_i|$, $3|M_i|$, and so on;
- similarly for $|M_{i+1}|$;
- all the points between the discrete lines (O, M_i) and (O, M_{i+1}) , and beyond the parallelogram $(O, M_i, M_{i+1}, M_i+M_{i+1})$ are obtained by using M_i or M_{i+1} .

Elementary displacements dx and dy from a point (x,y) are corresponding to the cost of a one square displacement (see Figure 2). We will now evaluate their values.

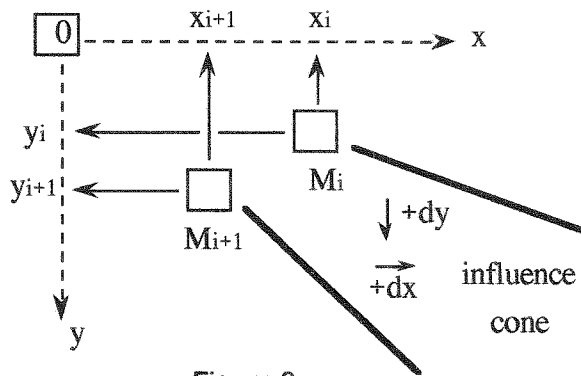


Figure 2.

Theorem 2:

If the points M_i/M_{i+1} are consecutive (i.e. if $x_i \cdot y_{i+1} - x_{i+1} \cdot y_i = 1$), then

- elementary displacements dx and dy are constant in the whole interior of the influence cone.
- their weights are given by

$$dx := y_{i+1} \cdot |M_i| - y_i \cdot |M_{i+1}|$$

$$dy := x_i \cdot |M_{i+1}| - x_{i+1} \cdot |M_i|$$

The second theorem is rigorously demonstrated in [12]. Hence we can say that chamfer masks are polygons with $8 \cdot (n-1)$ sides, and these sides are discrete lines, whose equations are defined by dx and dy .

Theorem 3:

A chamfer mask induces a distance if and only if, in each of its influence cones, the corresponding elementary displacements dx and dy , computed with theorem 2, respect the inequalities: $dx \geq dy \geq 0$ and $dx > 0$.

In a cone (M_i, M_{i+1}, dx, dy) we can state that $d_C = dy \cdot d_4 + (dx - dy) \cdot d_8$. Hence we deduce theorem 3 using the result that $u \cdot d_4 + v \cdot d_8$ is a distance if and only if $u \geq 0, v \geq 0, (u,v) \neq (0,0)$.

We emphasize the possibility to state directly the constraints for the affected points of the mask, by theorem 2 and 3:

$$dx \geq dy \geq 0 \text{ and } dx > 0 \Leftrightarrow$$

$$|M_i| \cdot (x_{i+1} + y_{i+1}) \geq |M_{i+1}| \cdot (x_i + y_i);$$

$$|M_{i+1}| \cdot x_i \geq |M_i| \cdot x_{i+1} \text{ and } |M_i| \cdot y_{i+1} > |M_{i+1}| \cdot y_i.$$

In other words, for any M_i et M_k where $y_i/x_i > y_k/x_k$

$$|M_i| \cdot \frac{x_k + y_k}{x_i + y_i} \geq |M_k| \geq |M_i| \cdot \frac{x_k}{x_i} \text{ and } |M_i| \cdot \frac{y_k}{y_i} > |M_k|$$

Application in 7×7 neighbourhood: we sort out by increasing angles with the line (Ox) points a-b-c-d-e, and we obtain:

name	M_i	x_i	y_i	$x_i + y_i$
a	M_1	1	0	1
d	M_2	3	1	4
c	M_3	2	1	3
e	M_4	3	2	5
b	M_5	1	1	2

According to theorem 3, an a-b-c-d-e mask will induce a distance only when the following inequalities are true:

$$4 \cdot a \geq d \geq 3 \cdot a \quad a > 0$$

$$9 \cdot d \geq 12 \cdot c \geq 8 \cdot d \quad d > c$$

$$10 \cdot c \geq 6 \cdot e \geq 9 \cdot c \quad 2 \cdot c > e$$

$$6 \cdot e \geq 15 \cdot b \geq 5 \cdot e \quad e > 2 \cdot b$$

General case: to compute a chamfer mask we choose a neighbourhood of visible points and the value $|M_1| = a$. Then we set for any point $M_i(x_i, y_i)$ ($i = 2..n$) of the mask the value $|M_i| = \text{Round}(a \cdot \sqrt{x_i^2 + y_i^2})$. It is very simple to find the a-values forbidden by theorem 3, depending on the size of the mask:

3*3	no one
5*5	2
7*7	1, 2, 3, 4, 6, 9
9*9	1, 2, 3, 4, 6, 9, 11, 16, 23
11*11	1, 2, 3, 4, 5, 6, 9, 11, 16, 21, 23, 26, 28, 33, 40

Every chamfer mask involving at least points a and b, whose affected points are all visible and weighted like described above, respects the inequalities of theorem 3 and thus infers a distance in mathematical sense if and only if the a-value is not forbidden.

3 - Optimizations

Chamfer distances can provide very good approximations of Euclidean distance, particularly the property of being isotropic. Several criteria can be used to compute chamfer masks.

G. Borgefors proposed in [4] that chamfer distances

approximate the Euclidean distance by resolving systems of inequations; she finds *float* intervals for a, b, c, .. values, and then computes fractions of integers b/a, c/a ... Finally the relative error is tested with regard to the Euclidean distance, on a vertical line limiting the discrete image.

This criterion is contested by J.H. Verwer in [13], who recommends to minimize the relative error on oblique lines or even Euclidean circles (which do not correspond any more with the image borders).

In these papers, the authors search *theoretical* values, and find the *upper limit* of errors; but they do not determine the *effective* errors on the discrete lattice. In discrete space the minimization criterion can be chosen among maximum of error, amplitude, or minimality on chamfer weights themselves. This latter is equivalent to minimize the errors on small distances; the two others walk on large distances. A way to unify the minimization is to process on the whole set of points of the picture (discrete integral).

We propose a new kind of optimization in [12]. Our purpose is to compute chamfer masks in larger neighbourhoods, and to minimize the *effective* errors on the image of integer distances (noted DT).

We know that chamfer disks are polygons, whose angles are supported by the assigned visible points in the mask. We will approximate the Euclidean circle with the *most regular polygons* we can find, choosing carefully the visible points to be affected, and then optimizing their value, according to one of the criteria above-mentioned.

Hence we check all the a-values from 2 to 255, calculating the weights of the choosen points p(x,y) of the mask with the formula $p := \text{round}(a \cdot \sqrt{x^2 + y^2})$, and finally we test the effective errors on the DT, on a vertical line limiting the picture.

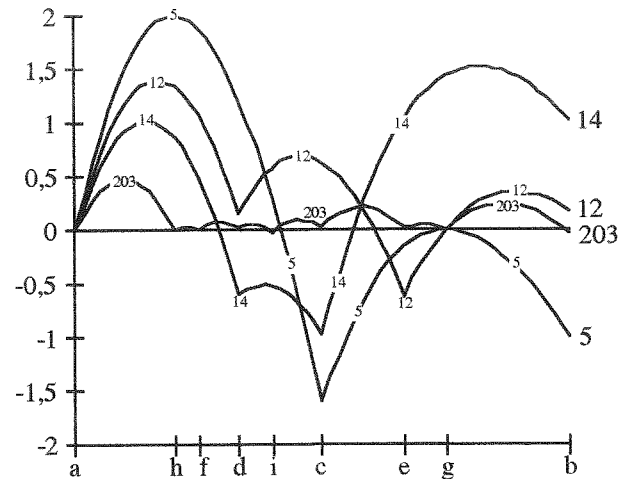


Figure 3.

Figure 3 shows that in a 7*7 kernel, 12-17-o-38-43 chamfer (o means that the value c=27 is removed) is better approximation than the Borgefors' chamfer 14-20-31-44. That is because a/d/e/b are better distributed than a/d/c/b in the first octant. Theorem 2 states that in both 38/27 and 27/43, dx and dy are equal (dx=11,dy=5), thus the c-value is not necessary.

Another example is chamfer 203-287-454-642-732-837-1015-1035-1093 in a 11*11 kernel whose maximum errors fall down to 0,47 % ! The resulting disk is a polygon with 64 sides, very close to the Euclidean circle (see Figure 4). The table below shows the progression (factor 100) from d4 to d203.. We can observe that the effective errors are not 8,09 % for 3-4 chamfer but 5,72 %, and not 2,02 % but 1,98 % for 5-7-11 chamfer (as it was announced in [4]).

distance	classic		G. Borgefors			E. Thiel	
	d4	d8	d3..	d5..	d14..	d12..	d203..
max error	41,42 %	29,29 %	5,72 %	1,98 %	1,52 %	1,38 %	0,48 %
amplitude	41,42 %	29,29 %	11,13 %	3,59 %	2,49 %	2,00 %	0,51 %

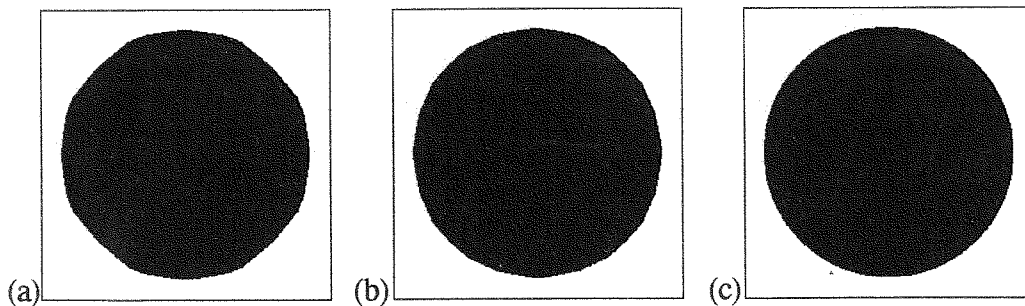


Figure 4. (a) d14.. (b) d12.. (c) d203..

4 - Results

Chamfer distances are very satisfactory considering the computing time of their distance transform, which requires only two sequential scanings of the picture, and with a discrete data structure (a matrix of 16-integers) [10].

Chamfer disk can be obtained by computing the appropriate distance transform on an 'infinite' size picture in which all the points are initially assigned to 1, except the center of the disk which is assigned to 0. A disk of radius R is the set of points whose value is lower than $R*a+r$, where a is the a -value of the mask and r belongs to $[0..a-1]$. For a fixed radius R there exists a family of a disks (when r varies) which induces a quasi-continuous way of going from the disk of radius R to the disk of radius $R+1$ (see Figure 5). This is of interest for animation, and discrete topology [1, 7, 9].

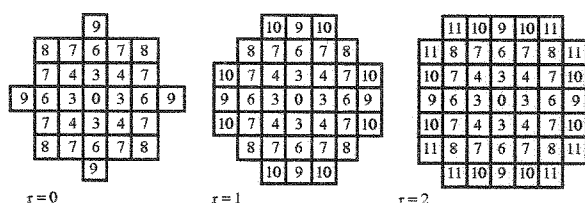


Figure 5. Chamfer 3-4 and $R = 3$

One of the most important applications of chamfers is the medial axis (a shape representation method) based on a covering of the shape by the maximal disks fitting in it [2]. The computation is very fast (only one scanning of the picture to identify the medial axis pixels). Of course the process is reversible, and allow to compute the medial line (a weighted skeleton) of the shape [3, 5, 11].

A very interesting application of this latter is shape splitting. Indeed a narrowing area which is detectable for a given metric squares with a neck point on the distance transformed picture. It is sufficient to traverse the medial line and to extract the local minima which do not locate at a tip. An efficient approach builds a symbolic representation of the original shape, and as the transformation is reversible, all the manipulations can be performed on this structure and are usually simple because they are some graph analysis processes.

The main contribution of chamfers with regard to d_g is to provide moreover isotropic distances: several narrowings undetectable with d_g will be detected with d_C .

Finally we mention an important contribution of chamfers in granulometry computation, in current use in material studies. Iterative methods based on mathematical morphology theory are usable, but the number of iterations depends on the width of the shape. A distance image enclose at the beginning the equivalent of the successive eroded pictures. As a comparison, a morphological granulometry endures 1h 30mn against 2mn using chamfer distances.

5 - Conclusion

In this paper we have proved that chamfer distances, under some conditions, are true distances in mathematical sense. This is important to justify the applications based on them, such as medial axes and medial lines.

We obtained some results concerning the geometry of chamfer disks, which provide new ways of understanding and optimizing chamfer masks on larger kernels.

The important point is that effective errors can now be computed directly in discrete space, and the choice of the assigned points is taken into account.

Finally we can state that chamfer distances provide very good approximations of the Euclidean distance and supply excellent alternatives to it. This study shows that the resulting quasi-isotropy is particularly effective for applications such as cytology or material studies.

Examples cited in § 4 are a few among the large field of applications, in which chamfers give substantial advantages in strength and efficiency.

6 - References

- [1] Eric ANDRES, "Cercles discrets et rotations discrètes", 1er coll. de géométrie discrète, CRI Strasbourg 91.
- [2] C. ARCELLI, G. SANNITI DI BAJA, "Finding local maxima in a pseudo-euclidean distance transform", CVGIP 43, p. 361-367, 1988.
- [3] C. ARCELLI, M. FRUCCI, "Reversible skeletonization by (5-7-11)-erosion", First International Workshop on Visual Form, May 27-30, 1991, Capri, Italy, published in Plenum Press, New York, 1992, p. 21-28.
- [4] G. BORGEFORS, "Distance transformations in digital images", CVGIP 34, p. 344-371, 1986.
- [5] J.M. CHASSERY, A. MONTANVERT, *Géométrie discrète en analyse d'images*, Ed. Hermès, 1991.
- [6] HARDY & WRIGHT, *An introduction to the theory of numbers*, Oxford University Press, fifth edition (october 1978), § III.3.1.
- [7] KOVALESKY V.A, "Finite Topology as applied to image analysis", CVGIP, 46, 1989, p.141-161.
- [8] U. MONTANARI, "A method for obtaining skeletons using a quasi-euclidean distance", J. of ACM vol 15 n°4, October 1968, p. 600-624.
- [9] J.P. REVELLES, "Géométrie Discrète, Calcul en Nombres Entiers et Algorithmique", Thèse U.L.P. Strasbourg, 1991.
- [10] A. ROSENFELD, J.L. PFALTZ, "Distance functions on digital pictures", Pattern Recognition, vol. 1, p. 33-61, 1968.
- [11] Edouard THIEL, Annick MONTANVERT, "Shape splitting from medial lines using the 3-4 chamfer distance", International Workshop on Visual Form, May 1991, Capri, published in Plenum Press, New York, 1992, p. 537-546.
- [12] E. THIEL, A. MONTANVERT, "Etude et amélioration des distances du chanfrein pour l'analyse d'images", revue TSI ed. Hermès, *vision par ordinateur*, 1992, to appear.
- [13] J.H. VERWER, "Local distance for distance transformations in two and three dimensions" Pattern Recognition Letters 12 (1991), p. 671-682.